



A thermodynamic potential for Ni₄₅Co₅Mn_{36.7}In_{13.3} single crystal

J. J. Wang, X. Q. Ma, H. B. Huang, W. Q. He, Z. H. Liu et al.

Citation: *J. Appl. Phys.* **114**, 013504 (2013); doi: 10.1063/1.4812741

View online: <http://dx.doi.org/10.1063/1.4812741>

View Table of Contents: <http://jap.aip.org/resource/1/JAPIAU/v114/i1>

Published by the [AIP Publishing LLC](#).

Additional information on *J. Appl. Phys.*

Journal Homepage: <http://jap.aip.org/>

Journal Information: http://jap.aip.org/about/about_the_journal

Top downloads: http://jap.aip.org/features/most_downloaded

Information for Authors: <http://jap.aip.org/authors>

ADVERTISEMENT



**Running in Circles Looking
for the Best Science Job?**

Search hundreds of exciting
new jobs each month!

<http://careers.physicstoday.org/jobs>

physicstodayJOBS



A thermodynamic potential for Ni₄₅Co₅Mn_{36.7}In_{13.3} single crystal

J. J. Wang,¹ X. Q. Ma,¹ H. B. Huang,^{1,2} W. Q. He,¹ Z. H. Liu,¹ and Long-Qing Chen²

¹Department of Physics, University of Science and Technology Beijing, Beijing 100083, China

²Department of Materials Science and Engineering, Pennsylvania State University, University Park, Pennsylvania 16802, USA

(Received 29 May 2013; accepted 17 June 2013; published online 1 July 2013)

A thermodynamic potential as a function of the ferromagnetic, antiferromagnetic, and martensite order parameters is developed using existing experimental data. It successfully reproduces the single domain properties of Ni₄₅Co₅Mn_{36.7}In_{13.3} bulk crystal, including the Curie temperature, the transition temperature from ferromagnetic austenite phase to antiferromagnetic martensite phase as well as its response to an externally applied magnetic field, the saturated magnetization, the martensite strain, the entropy change, and the magnetic permeability. It can be applied to explore the stress-strain and magnetic field-strain behaviors and implemented in phase field simulations to study the ferromagnetic, antiferromagnetic, and martensite domain stability and evolution.

© 2013 AIP Publishing LLC. [<http://dx.doi.org/10.1063/1.4812741>]

There has been significant progress in refrigeration since the discovery of the magnetocaloric effect (MCE).¹ The idea of cooling via adiabatic demagnetization is proposed by Debye² and Giauque.³ The discovery of giant MCE (GMCE) in Gd₅Si₂Ge₂ demonstrated that magnetic refrigeration is a promising and competitive cooling technology,⁴ and thus, there have been increasing interests in search for new GMCE materials. The ferromagnetic shape-memory alloys are candidate GMCE materials since magnetic and structural transitions occur nearly simultaneously. Indeed, the Co-doped Ni-Mn-In (Ni₄₅Co₅Mn_{36.6}In_{13.4}) alloys were reported to show much more sensitive response of the transition temperature, from ferromagnetic austenite phase to antiferromagnetic martensite phase, to an external magnetic field than pure Ni-Mn-In alloys.⁵ Several similar alloys such as Ni-Co-Mn-In,⁶ Ni-Co-Mn-Sn,⁷ Ni-Co-Mn-Sb,⁸ Ni-Co-Mn-Ga,⁹ and even their Cu-coped counterparts^{10–12} have also been investigated for the magnetocaloric effect.

In addition to the experimental studies, first principle calculation¹³ was performed to understand the phase stabilities of the shape memory alloy Ni₂MnGa in which the ferromagnetic phase and martensite phase coexist. Based on the Landau phenomenological theory,^{14,15} the phase field model has been employed to understand the ferromagnetic domain structures, martensite domain structures, stress-strain

behaviors, and magnetic field-strain behaviors.^{16–20} Phase field model requires the thermodynamic potential as an input. However, for Ni-Co-Mn-In alloys, there is still no available thermodynamic potential with a complete set of coefficients although a thermodynamic free energy model has been proposed by Buchel'nikov *et al.* to analyze the phase stabilities qualitatively.²¹ Therefore, to quantitatively analyze the effects of external fields on phase transition temperatures and various physical properties of Ni-Co-Mn-In alloys as well as to carry out phase-field simulations of domain evolution in these alloys under external fields require a thermodynamic potential with a complete set of coefficients. In this work, based on the existing experimental measurements for magnetic and structural properties for Ni₄₅Co₅Mn_{36.6}In_{13.4} alloys, we constructed a complete thermodynamic potential by fitting the coefficients to the experimental data.

It has been known from experiments that by decreasing the temperature from the Curie point, Ni₄₅Co₅Mn_{36.6}In_{13.4} bulk crystal undergoes a phase transition from the paramagnetic austenite phase to the ferromagnetic austenite phase at about 400 K, and a phase transition from ferromagnetic austenite phase to antiferromagnetic martensite phase at about 285 K.^{5,22} For a Ni₄₅Co₅Mn_{36.6}In_{13.4} single crystal, the total free energy can be written in the following form:²¹

$$\begin{aligned} \Delta f = & \alpha_1 \mathbf{M}^2 + \alpha_{11} (M_x^4 + M_y^4 + M_z^4) + \alpha_{12} (M_x^2 M_y^2 + M_x^2 M_z^2 + M_y^2 M_z^2) + \alpha_{112} [M_x^2 (M_y^2 + M_z^2) + M_y^2 (M_x^2 + M_z^2) + M_z^2 (M_x^2 + M_y^2)] \\ & + \alpha_{111} (M_x^6 + M_y^6 + M_z^6) + \alpha_{123} M_x^2 M_y^2 M_z^2 + \beta_1 \mathbf{L}^2 + \beta_{11} (L_x^4 + L_y^4 + L_z^4) + \beta_{12} (L_x^2 L_y^2 + L_x^2 L_z^2 + L_y^2 L_z^2) \\ & + \beta_{112} [L_x^2 (L_y^2 + L_z^2) + L_y^2 (L_x^2 + L_z^2) + L_z^2 (L_x^2 + L_y^2)] + \beta_{111} (L_x^6 + L_y^6 + L_z^6) + \beta_{123} L_x^2 L_y^2 L_z^2 \\ & + \mu_{11} (\mathbf{M} \cdot \mathbf{L})^2 + \mu_{12} \mathbf{M}^2 \mathbf{L}^2 - (M_x H_x + M_y H_y + M_z H_z) + Q_1 e_1^2 + Q_2 (e_2^2 + e_3^2) + Q_3 (e_4^2 + e_5^2 + e_6^2) \\ & + Q_4 e_1 (e_2^2 + e_3^2) + Q_5 e_3 (e_3^2 - 3e_2^2) + Q_6 (e_2^2 + e_3^2)^2 + \gamma_0 e_1 \mathbf{M}^2 + \gamma_1 [e_2 (M_x^2 - M_y^2)/2 + e_3 (3M_z^2 - \mathbf{M}^2)/\sqrt{6}] \\ & + \gamma_2 (e_4 M_x M_y + e_5 M_y M_z + e_6 M_x M_z) + \lambda_0 e_1 \mathbf{L}^2 + \lambda_1 [e_2 (L_x^2 - L_y^2)/2 + e_3 (3L_z^2 - \mathbf{L}^2)/\sqrt{6}] + \lambda_2 (e_4 L_x L_y + e_5 L_y L_z + e_6 L_x L_z), \end{aligned} \quad (1)$$

where $\mathbf{M} = (\mathbf{M}_1 - \mathbf{M}_2)/2M_S$ and $\mathbf{L} = (\mathbf{M}_1 + \mathbf{M}_2)/2M_S$ are the normalized ferromagnetic and antiferromagnetic vectors with \mathbf{M}_1 and \mathbf{M}_2 the sublattice magnetization vectors; $\alpha_1, \alpha_{11}, \alpha_{12}, \alpha_{111}, \alpha_{112}, \alpha_{123}, \beta_1, \beta_{11}, \beta_{12}, \beta_{111}, \beta_{112}, \beta_{123}, \mu_{11},$ and μ_{12} are Landau potential coefficients which can be fitted using the bulk properties of the single crystal,^{5,22} similar to a procedure used in ferroelectrics;²³ $\mathbf{H} = (H_x, H_y, H_z)$ is the external magnetic field vector, e_i are the linear combination of the strain tensor components, $e_1 = (\epsilon_{xx} + \epsilon_{yy} + \epsilon_{zz})/\sqrt{3}$, $e_2 = (\epsilon_{xx} - \epsilon_{yy})/\sqrt{2}$, $e_3 = (2\epsilon_{zz} - \epsilon_{xx} - \epsilon_{yy})/\sqrt{6}$, $e_4 = \epsilon_{xy}$, $e_5 = \epsilon_{yz}$, $e_6 = \epsilon_{zx}$; $Q_1, Q_2, Q_3, Q_4, Q_5, Q_6$ are the linear combinations of the second-, third-, and fourth-order elastic moduli, respectively, $Q_1 = (c_{11} + 2c_{12})/2\sqrt{3}$, $Q_2 = (c_{11} - c_{12})/2$, $Q_3 = c_{44}$, $Q_4 = (c_{111} - c_{123})/2\sqrt{3}$, $Q_5 = (c_{111} - 3c_{112} + 2c_{123})/18\sqrt{6}$, $Q_6 = (c_{1111} + c_{1112} - 3c_{1122} - 8c_{1123})/192$; and $\gamma_0, \gamma_1, \gamma_2, \lambda_0, \lambda_1, \lambda_2$ are the magnetostrictive parameters. In this work, we assumed that the $\text{Ni}_{45}\text{Co}_5\text{Mn}_{36.7}\text{In}_{13.3}$ has the same structural transition from $L2_1$ to $L1_0$ as $\text{Ni}_8\text{Mn}_6\text{In}_2$ alloy,²⁴ thus, γ_2 and λ_2 can be neglected because of the disappearance of shear strain during the phase transition. Table I shows all the coefficients obtained in this work. Due to the lack of enough experimental data, some of the needed coefficients are estimated in order to reproduce the experimentally observed phase transitions and physical properties.

Using the fitted potential, we calculated the magnetic and structural properties of $\text{Ni}_{45}\text{Co}_5\text{Mn}_{36.7}\text{In}_{13.3}$ single crystal by minimizing the total free energy density in Eq. (1). Figure 1 shows the total magnetization variation with temperature under different magnitude of magnetic field. It can be seen from Figure 1 that under zero magnetic field $\text{Ni}_{45}\text{Co}_5\text{Mn}_{36.7}\text{In}_{13.3}$ undergoes two magnetic phase transitions as temperature decreases, i.e., a first order phase transition from paramagnetic phase to ferromagnetic phase at 402 K and another first order phase transition from ferromagnetic phase to antiferromagnetic phase at 284 K, which agree well with existing experimental measurements (Table II).

According to the thermodynamic potential, the phase transition from paramagnetic phase to ferromagnetic phase becomes second order under an applied magnetic field, while the phase transition from ferromagnetic phase to antiferromagnetic remains to be first order.

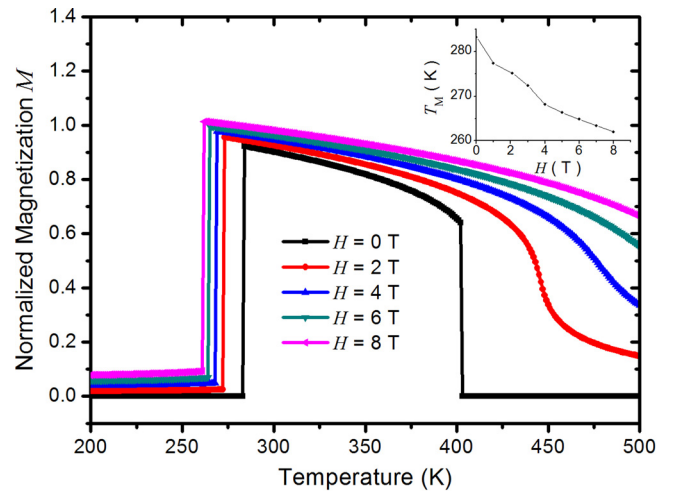


FIG. 1. Magnetization of $\text{Ni}_{45}\text{Co}_5\text{Mn}_{36.7}\text{In}_{13.3}$ single crystal vs temperature at different magnetic field, the inset shows the transition temperature at different magnetic field.

The transition temperature from ferromagnetic phase to antiferromagnetic phase decreases markedly with increasing applied magnetic field at a ratio of -4 K/T when the applied magnetic field is smaller than 4 T. Comparable values, -4.2 K/T and -9 K/T, were obtained in experiments^{5,25} (Table II). These values are significantly larger than that of classical Ni-Mn-Ga alloys.

Figure 2 shows the variation of strain components with temperature under different magnitude of magnetic field. A structural phase transition from austenite phase (cubic symmetry) to martensite phase (tetragonal symmetry) takes place as temperature is lowered and the transition temperature decreases with magnetic field increasing. In our model, the antiferromagnetic phase and martensite structure co-exist below the transition temperature under a stress-free boundary condition. The coexistence of antiferromagnetic and martensite phases arises from the magnetostrictive interactions described by the γ_i and λ_i terms in Eq. (1).

According to our calculations, the tetragonality c/a of $\text{Ni}_{45}\text{Co}_5\text{Mn}_{36.7}\text{In}_{13.3}$ single crystal at 0 K is about 1.15, by comparison with a value of 1.30 from first principle calculation for $\text{Ni}_8\text{Mn}_6\text{In}_2$ single crystal²⁴ (Table II). Additionally,

TABLE I. Coefficients in Eq. (1) obtained in this work, where T is temperature in Kelvin.

Coefficients	This work	Unit	Coefficients	This work	Unit
α_1	$4.104 \times 10^4 \times (T - 382)$	J/m ³	μ_{11}	2.000×10^7	J/m ³
α_{11}	-4.099×10^6	J/m ³	μ_{12}	2.000×10^7	J/m ³
α_{12}	4.200×10^6	J/m ³	Q_1	1.110×10^{12}	J/m ³
α_{111}	5.060×10^6	J/m ³	Q_2	$2.8 \times 10^8 \times (T - 245)$	J/m ³
α_{112}	9.520×10^6	J/m ³	Q_3	7.700×10^{10}	J/m ³
α_{123}	5.770×10^7	J/m ³	Q_4	4.000×10^{10}	J/m ³
β_1	$1.200 \times 10^5 \times (T - 290)$	J/m ³	Q_5	-2.500×10^{11}	J/m ³
β_{11}	-1.700×10^7	J/m ³	Q_6	4.000×10^{12}	J/m ³
β_{12}	1.740×10^7	J/m ³	γ_0	1.000×10^7	J/m ³
β_{111}	1.800×10^7	J/m ³	γ_1	2.000×10^6	J/m ³
β_{112}	4.914×10^7	J/m ³	λ_0	1.000×10^8	J/m ³
β_{123}	2.978×10^8	J/m ³	λ_1	-2.500×10^8	J/m ³

TABLE II. Saturated magnetization M_S , tetragonality c/a , entropy change ΔS , Curie temperature T_C , transitional temperature T_M and its response to external magnetic field $\left(\frac{dT_M}{dH}\right)_H$, and magnetic permeability μ_c from different sources.

Properties	This work	Experiment or first principle
Magnetization (at 263 K, 7 T)	6.33×10^5 (A/m)	6.88 ^a
Tetragonality c/a (at 0 K, 0 T)	1.15	1.30 (For $\text{Ni}_8\text{Mn}_6\text{In}_2$), ^b 1.17 ^c
ΔS (at 273 K, 2 T)	14.93 (J/kg · K)	15.2, ^a 4.7 ^d
T_C (at 0 T)	402 K	382, ^a 375, ^e 402 ^e
T_M (at 0 T)	284 K	282, ^a 328, ^e 248 ^e
Permeability μ_c (at 300 K, 1 T)	4.2×10^{-3} ($\mu_B/\text{f.u.}$)	0.02 ^e
$\left(\frac{dT_M}{dH}\right)_H$ (at 4 T)	4.0 (K/T)	4.2, ^a 9.0 ^d

^aReference 5.

^bReference 24.

^cReferences 6 and 26.

^dReference 25.

^eReference 22.

from both the magnetization and strain changes at the transition temperature, we can see that the the martensite phase transition remains to be first order even though at nonzero applied magnetic field.

The relative magnetic stiffness is deduced from the second-order derivatives of the free energy function with respect to the magnetization, i.e., $\chi_{ij} = \mu_0 \frac{\partial^2 \Delta f}{\partial M_i \partial M_j}$, and the relative magnetic permeability can be obtained by making a coordinate transformation. By using the same coordinate transformation in previous work on BaTiO_3 system,²³ we calculated the relative magnetic permeability variation with temperature under an applied magnetic field 1 T along [001] direction, as shown in Figure 3. It can be seen from the calculation that the permeability along the magnetic field is weaker than perpendicular to the magnetic field. We converted some results of Ito *et al.*'s work in order to make comparison with our calculated result,²² as shown in Figure 3, and we can see that our calculated result is a slightly smaller than the experimental result.

$\text{Ni}_{45}\text{Co}_5\text{Mn}_{36.7}\text{In}_{13.3}$ alloys exhibit excellent magneto-caloric effect as a result of the abrupt change in the

magnetization through the martensite phase transition which can induce large entropy change. According to classical thermodynamics, the entropy change $\Delta S(T, H)$ can be indirectly determined by using the following formula:

$$\Delta S(T, H) = S(T, H) - S(T, 0) = \mu_0 \int_0^H \left(\frac{\partial M(T)}{\partial T} \right)_H dH. \quad (2)$$

Figure 4 shows the entropy change ΔS of $\text{Ni}_{45}\text{Co}_5\text{Mn}_{36.7}\text{In}_{13.3}$ single crystal varying with temperature at different maximum applied magnetic field. It can be seen that entropy change due to the simultaneously magnetic and structural phase transitions reaches a value of 14.93 J/(kg·K) under a maximal magnetic field of 2 T, which agrees well with the experimental value of 15.2 J/(kg·K), as shown in Table II.

In summary, a thermodynamic potential of $\text{Ni}_{45}\text{Co}_5\text{Mn}_{36.7}\text{In}_{13.3}$ single crystal was constructed. The properties determined from the thermodynamic potential and the corresponding experimental values show excellent agreements, including the Curie temperature, transitional

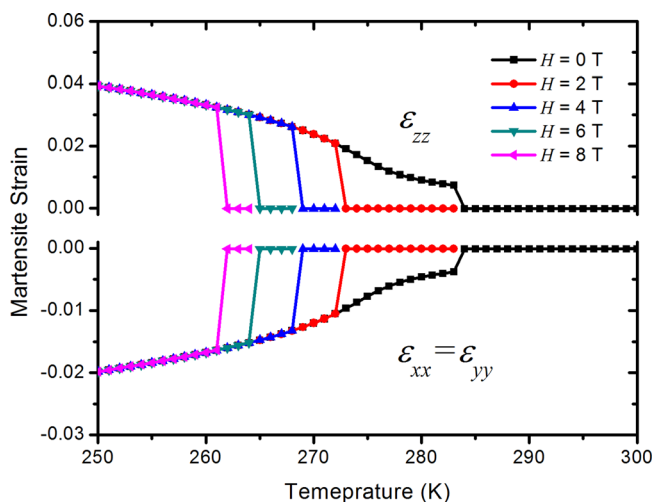


FIG. 2. Martensite strain of $\text{Ni}_{45}\text{Co}_5\text{Mn}_{36.7}\text{In}_{13.3}$ single crystal vs temperature at different magnetic field, each step indicates a martensite phase transition.

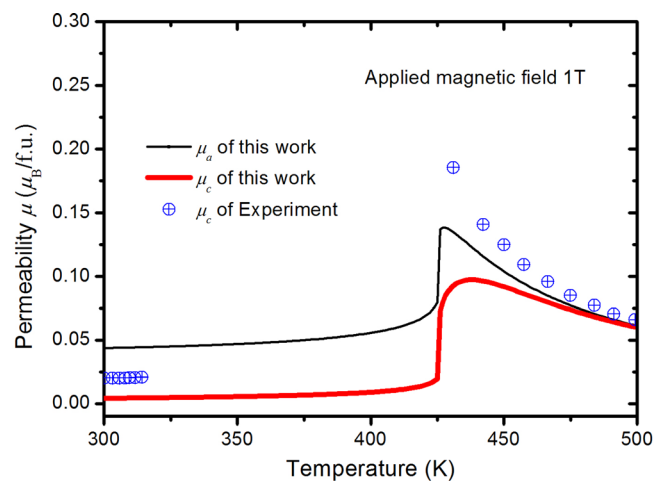


FIG. 3. Magnetic permeability of $\text{Ni}_{45}\text{Co}_5\text{Mn}_{36.7}\text{In}_{13.3}$ single crystal vs temperature with applied magnetic field 1 T, the experimental data was partly transformed from Ito *et al.*'s work.²²

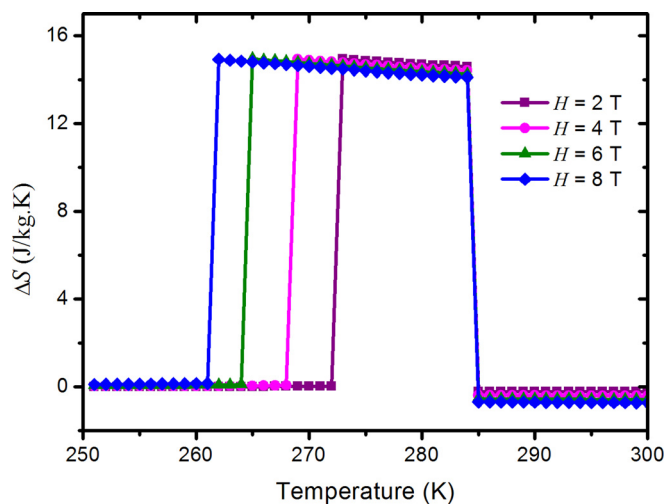


FIG. 4. Entropy change ΔS of $\text{Ni}_{45}\text{Co}_5\text{Mn}_{36.7}\text{In}_{13.3}$ single crystal vs temperature for different maximum applied magnetic field.

temperature from ferromagnetic austenite phase to antiferromagnetic martensite phase and its response to the external magnetic field, saturated magnetization, tetragonality c/a , entropy change, and magnetic permeability. The quantitative depiction of the thermodynamic free energy using the fitted coefficients embedded in the phase field mode provides a way to predict the magnetic and structural properties of $\text{Ni}_{45}\text{Co}_5\text{Mn}_{36.7}\text{In}_{13.3}$ alloys.

This work was partially supported by National Science Foundation of China under Grant No. 11174030 and US NSF under Grant No. DMR-1006541. The computations were performed in University of Science and Technology Beijing, China and partially using the LION and Cyberstar clusters at the Pennsylvania State University supported in part by NSF Major Research Instrumentation Program through Grant No. OCI-0821527 and in part by the Materials Simulation Center and the Graduated Education and Research Services at the Pennsylvania State University.

- ¹E. Warburg, *Ann. Phys.* **249**, 141 (1881).
- ²P. Debye, *Ann. Phys.* **386**, 1154 (1926).
- ³W. F. Giauque, *J. Am. Chem. Soc.* **49**, 1864 (1927).
- ⁴V. K. Pecharsky and J. K. A. Gschneidner, *Phys. Rev. Lett.* **78**, 4494 (1997).
- ⁵R. Kainuma, Y. Imano, W. Ito, Y. Sutou, H. Morito, S. Okamoto, O. Kitakami, K. Oikawa, A. Fujita, and T. Kanomata, *Nature* **439**, 957 (2006).
- ⁶Y. D. Wang, E. W. Huang, Y. Ren, Z. H. Nie, G. Wang, Y. D. Liu, J. N. Deng, H. Choo, P. K. Liaw, D. E. Brown, and L. Zuo, *Acta Mater.* **56**, 913 (2008).
- ⁷K. Ito, W. Ito, R. Y. Umetsu, M. Nagasako, R. Kainuma, A. Fujita, K. Oikawa, and K. Ishida, *Mater. Trans.* **49**, 1915 (2008).
- ⁸S. Y. Yu, L. Ma, G. D. Liu, Z. H. Liu, J. L. Chen, Z. X. Cao, G. H. Wu, B. Zhang, and X. X. Zhang, *Appl. Phys. Lett.* **90**, 242501 (2007).
- ⁹S. Y. Yu, Z. X. Cao, L. Ma, G. D. Liu, J. L. Chen, G. H. Wu, B. Zhang, and X. X. Zhang, *Appl. Phys. Lett.* **91**, 102507 (2007).
- ¹⁰C. B. Jiang, J. M. Wang, P. P. Li, A. Jia, and H. B. Xu, *Appl. Phys. Lett.* **95**, 012501 (2009).
- ¹¹B. Gao, J. Shen, F. X. Hu, J. Wang, J. R. Sun, and B. G. Shen, *Appl. Phys. A Mater. Sci. Process.* **97**, 443 (2009).
- ¹²V. K. Sharma, M. K. Chattopadhyay, A. Khandelwal, and S. B. Roy, *Phys. Rev. B* **82**, 172411 (2010).
- ¹³M. A. Uijttewaalt, T. Hickel, J. Neugebauer, M. E. Gruner, and P. Entel, *Phys. Rev. Lett.* **102**, 35702 (2009).
- ¹⁴E. Hoffmann, H. Herper, P. Entel, S. G. Mishra, P. Mohn, and K. Schwarz, *Phys. Rev. B* **47**, 5589 (1993).
- ¹⁵F. Falk, *Acta Metall.* **28**, 1773 (1980).
- ¹⁶J. X. Zhang and L. Q. Chen, *Philos. Mag. Lett.* **85**, 533 (2005).
- ¹⁷Y. M. M. Jin, *Acta Mater.* **57**, 2488 (2009).
- ¹⁸P. P. Wu, X. Q. Ma, J. X. Zhang, and L. Q. Chen, *J. Appl. Phys.* **104**, 073906 (2008).
- ¹⁹P. P. Wu, X. Q. Ma, J. X. Zhang, and L. Q. Chen, *Philos. Mag.* **91**, 2102 (2011).
- ²⁰L. J. Li, J. Y. Li, Y. C. Shu, H. Z. Chen, and J. H. Yen, *Appl. Phys. Lett.* **92**, 172504 (2008).
- ²¹V. D. Buchel'nikov, S. V. Taskaev, M. A. Zagrebin, and P. Entel, *JETP Lett.* **85**, 560 (2007).
- ²²W. Ito, M. Nagasako, R. Y. Umetsu, R. Kainuma, T. Kanomata, and K. Ishida, *Appl. Phys. Lett.* **93**, 232503 (2008).
- ²³J. J. Wang, P. P. Wu, X. Q. Ma, and L. Q. Chen, *J. Appl. Phys.* **108**, 114105 (2010).
- ²⁴P. Entel, S. Sahoo, M. Siewert, M. E. Gruner, H. C. Herper, D. Comtesse, M. Acet, V. D. Buchel'nikov, and V. V. Sokolovskiy, *AIP Conf. Proc.* **1461**, 11 (2012).
- ²⁵V. Recarte, J. I. Perez-Landazabal, S. Kustov, and E. Cesari, *J. Appl. Phys.* **107**, 053501 (2010).
- ²⁶Y. D. Wang, Y. Ren, E. W. Huang, Z. H. Nie, G. Wang, Y. D. Liu, J. N. Deng, L. Zuo, H. Choo, P. K. Liaw, and D. E. Brown, *Appl. Phys. Lett.* **90**, 101917 (2007).